ADVANCED OPTICAL MATERIALS

Supporting Information

for *Adv. Optical Mater.,* DOI: 10.1002/adom.202102263

GaN-Based Deep-Nano Structures: Break the Efficiency Bottleneck of Conventional Nanoscale Optoelectronics

*Ishtiaque Ahmed Navid, Ayush Pandey, Yin Min Goh, Jonathan Schwartz, Robert Hovden, and Zetian Mi**

GaN-based Deep-Nano Structures: Break the Efficiency Bottleneck of Conventional Nanoscale Optoelectronics

Ishtiaque Ahmed Navid[1], Ayush Pandey[1], Yin Min Goh[2], Jonathan Schwartz[2], Robert Hovden[2], and Zetian Mi[1*]

[1]*Department of Electrical Engineering and Computer Science, University of Michigan, Ann Arbor, 1301 Beal Avenue, Ann Arbor, MI 48109, USA*

[2]*Department of Materials Science and Engineering, University of Michigan, Ann Arbor,* 2300 Hayward St, *Ann Arbor, MI 48109, USA*

[*] *Corresponding author E-mail: ztmi@umich.edu; Phone: 1 734 764 3963*

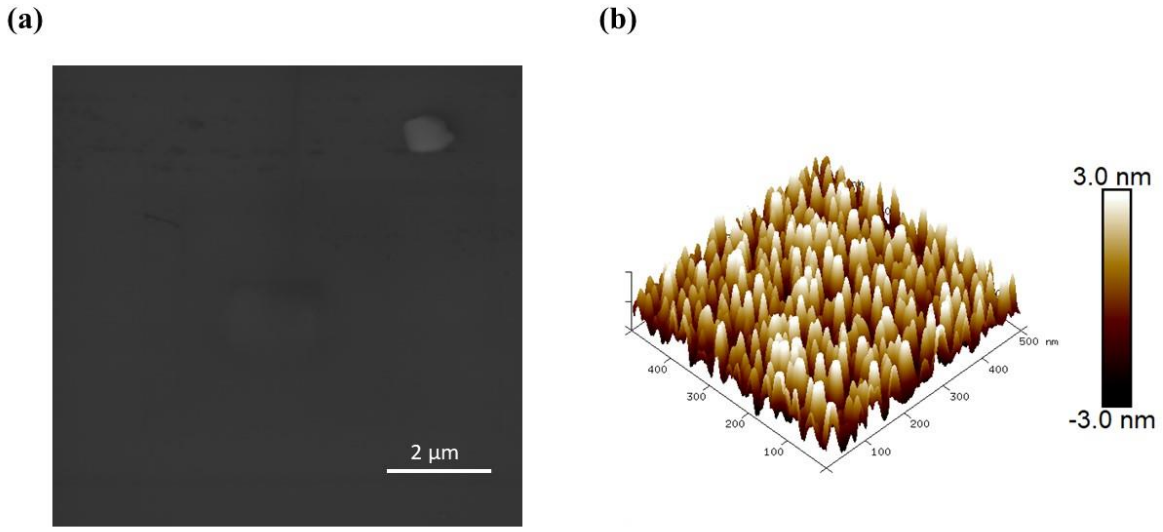

Figure S1. (a) SEM and (b) AFM images of AlN buffer layer grown for 5 mins on Si (111) substrate.

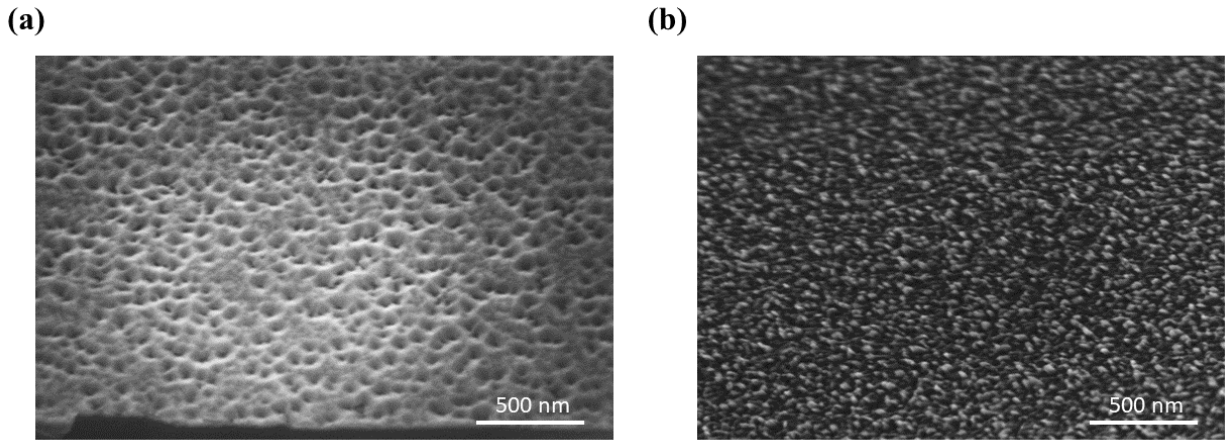

Figure S2. SEM images at 45^{o} tilt angle of initial GaN nanostructure morphology (growth duration of 20mins) on (a) AlN buffer layer and (b) bare Si (111) substrate, showing the presence of micro-network and nanowire-like morphology, respectively.

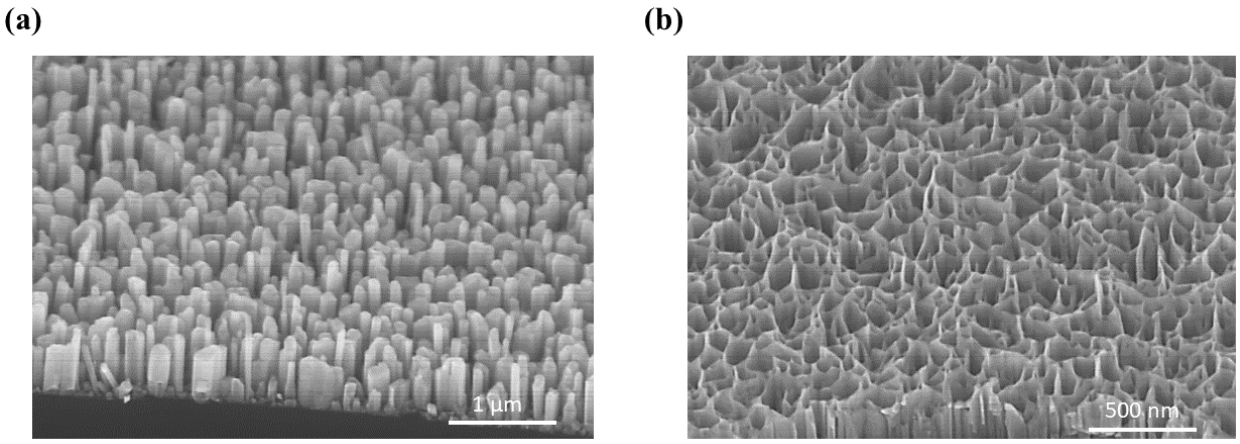

Figure S3. SEM images at 45^{o} tilt angle of (a) GaN nanowires grown for 2 hrs on bare Si (111) substrate and (b) GaN micro-network nanostructures grown for 2 hr on ~2 nm thick AlN buffer layer. The same growth conditions were used in both cases. Here the morphology difference arises due to the presence of the AlN buffer layer.

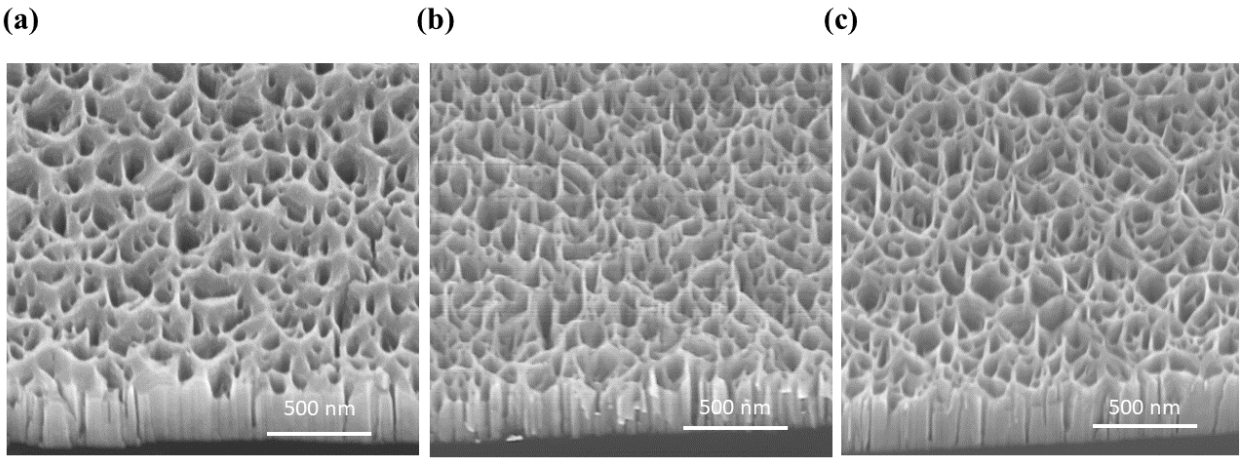

Figure S4. SEM images at 45^{o} tilt angle of GaN micro-network nanostructures grown with (a) 0.5 sccm, (b) 1 sccm, and (c) 1.5 sccm N_2 flow on Si (111) substrate with AlN buffer layer.

Figures S4 and S5 show the SEM images of GaN micro-network grown under various conditions. It is seen that such micro-network nanostructures can be formed under a wide range of epitaxy conditions. Figures S4 (a)-(c) depict the morphology of GaN micro-networks grown at N_2 flow rates of 0.5 sccm, 1 sccm and 1.5 sccm, respectively, with the substrate temperature at 755 ^{o}C. It is observed that the micro-network lateral widths and growth rates vary with different N_2 flow rates. For 0.5 sccm, 1 sccm and 1.5 sccm N_2 flow rates, the micro-network nanostructure lateral widths are nominally ~42 nm, ~30 nm and ~18 nm, respectively, whereas the growth rates are ~52 nm/hr, 71 nm/hr and 80 nm/hr, respectively. As such, it is clear that a higher N_2 flow rate promotes the vertical growth of the GaN micro-network but suppresses the lateral adatom migration.[1] Moreover, Figures S5 (a)-(c) show the impact of substrate temperature variation on the GaN micro-network nanostructure morphology at 670 ^{o}C, 710 ^{o}C and 790 ^{o}C, respectively. The N_2 flow rate was kept at 1.5 sccm for these samples. For the growth temperatures of 670 ^{o}C, 710 ^{o}C and 790 ^{o}C, the micro-network nanostructure hole diameters are found to be ~27 nm, ~45 nm and ~89 nm, respectively, while the growth rates are ~60 nm/hr, 73 nm/hr and 81 nm/hr, respectively. Larger hole diameters imply smaller micro-network nanostructure lateral widths. Therefore, at an elevated growth temperature, the GaN micro-network nanostructure vertical growth is enhanced with suppressed lateral growth.[2]

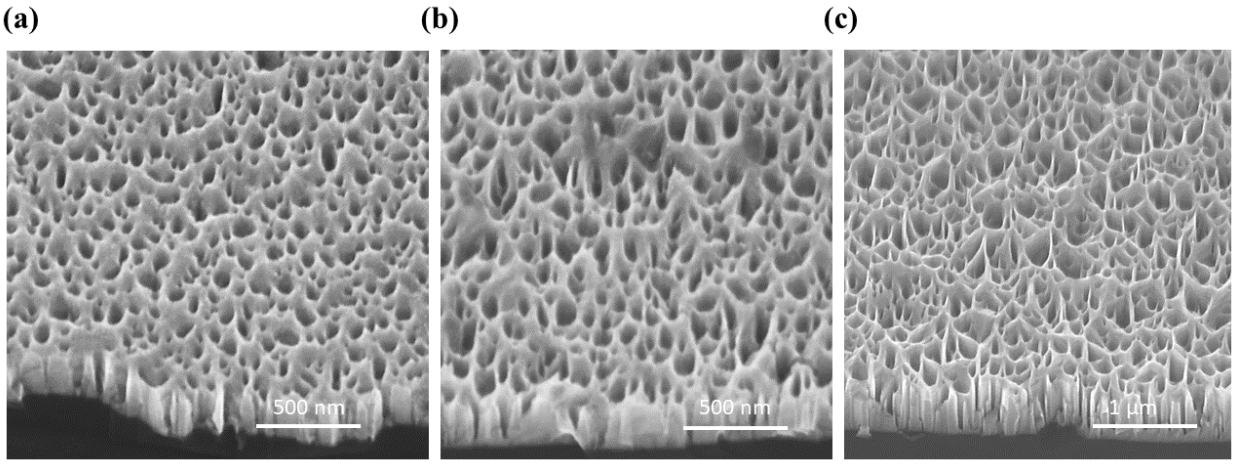

Figure S5. SEM images at 45^{o} tilt angle of GaN micro-network nanostructures grown with (a) 670 ^{o}C, (b) 710 ^{o}C, and (c) 790 ^{o}C substrate temperatures on Si (111) substrate with AlN buffer layer.

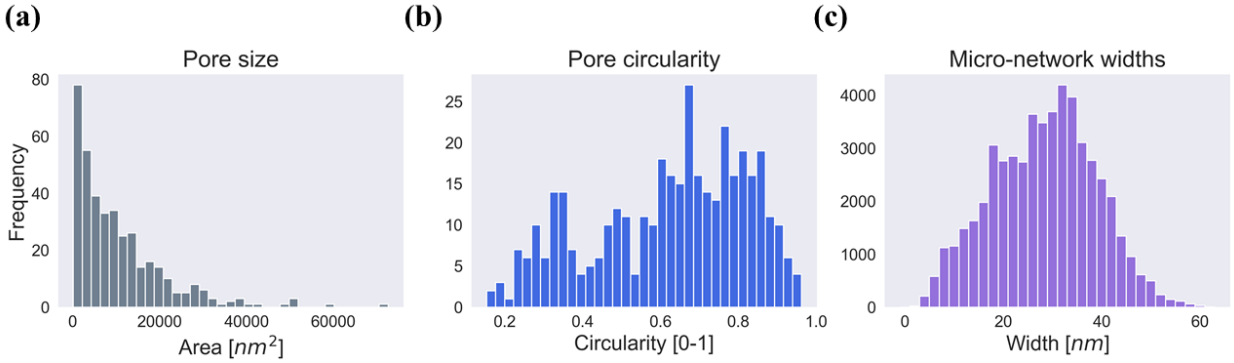

Figure S6. Graphical representation for the distribution of micro-network (a) pore size, (b) pore circularity, and (c) width.

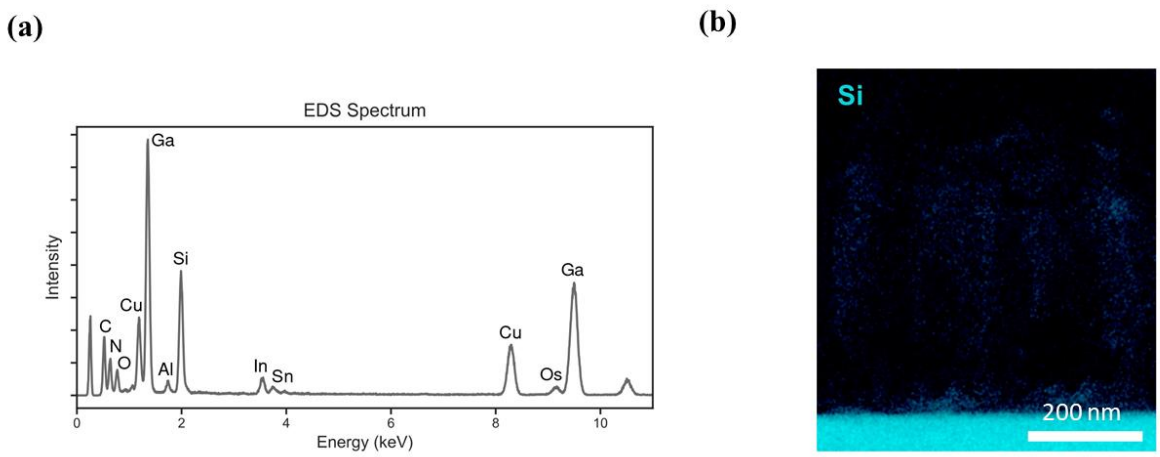

Figure S7. (a) Energy-dispersive X-ray spectrum (EDS) of InGaN micro-network nanostructures and (b) Elemental mapping of Si substrate.

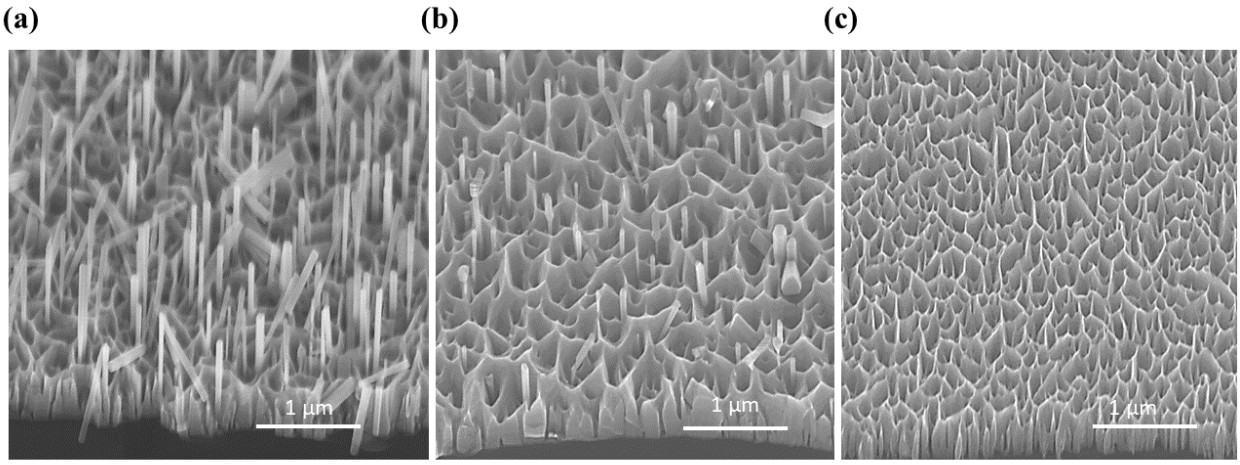

Figure S8. SEM images at 45^{o} tilt angle of InGaN micro-network nanostructures growth with (a) 755 ^{o}C, (b) 675 ^{o}C, and (c) 600 ^{o}C substrate temperatures on Si (111) substrate with AlN buffer layer.

We have further studied the effect of growth parameters on the formation and properties of InGaN micro-network nanostructures. Shown in Figure S8(a)-(c) are the SEM images of InGaN micro-networks grown under different growth temperatures at 755 ^{o}C, 675 ^{o}C and 600 ^{o}C,

respectively. From Figure S8(a), it is seen that substrate temperature of 755 ^{o}C results in the mixture of InGaN nanowires and micro-network morphology with micro-network growth rate of ~92 nm/hr. The formation of nanowire structure here indicates the promotion of the vertical migration of the adatoms under N_2 rich conditions at high substrate temperatures. Also from the photoluminescense (PL) spectrum, only the GaN PL peak at ~365 nm was dominant,[3] implying the In adatom desorption from the micro-network surface at high substrate temperature due to its low sticking coefficient.[4] At 675 ^{o}C substrate temperature, the formation of the nanowire structures is less pronounced (Figure S8(b)) with a growth rate of ~85 nm/hr. A lower substrate temperature of 600 ^{o}C completely eliminates the nanowire formation with a micro-network growth rate of ~73 nm/hr, which was found to be the optimum window of the growth temperature (Figure S8(c)).

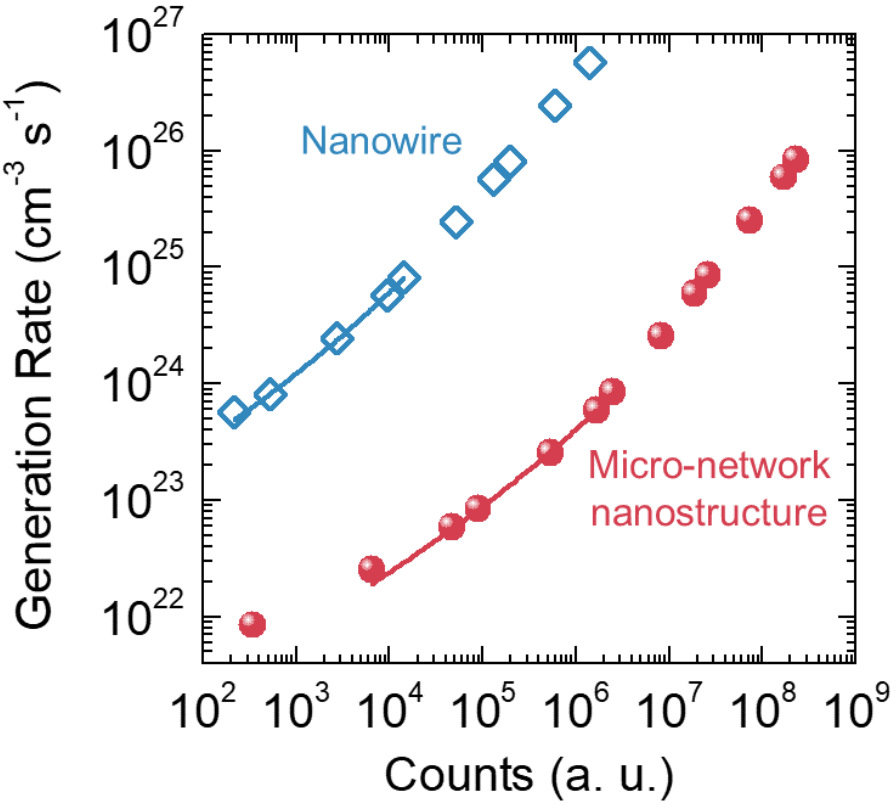

Figure S9. Generation rate versus intensity counts for InGaN micro-network nanostructure and conventional nanowires.

The generation rate was calculated for the different excitation intensities, assuming a fill factor of 75% for both the micro-network nanostructures and nanowires, an InGaN composition of 33%, and an absorption coefficient α of 10^5 cm^{-1}, based on previous parameters.[5] From the rate equations, the generation rate G and the detected counts I are given by:[6]

$$G = An + Bn^2 + Cn^3$$

$$I = \theta Bn^2$$

where A is the non-radiative Shockley-Read-Hall (SRH) recombination coefficient, B is the radiative recombination coefficient, C is the Auger recombination coefficient, n is the carrier

density, and θ is a constant determined by the setup. By considering only the points at low excitation powers, before the onset of the droop in relative EQE, the Auger recombination coefficient can be neglected in the analysis of the rate equations. By fitting the G vs I curve (the fit is the red guideline), shown in the of Figure S9, the parameter $\frac{A}{\sqrt{B}}$ can be extracted. The values for $\frac{A}{\sqrt{B}}$ are 5.2×10^{11} $cm^{-1.5}$ $s^{-0.5}$ and 1.6×10^{12} $cm^{-1.5}$ $s^{-0.5}$ for the micro-network nanostructure and the conventional nanowire samples, respectively. Assuming that both samples have comparable radiative recombination coefficients due to the similar InGaN compositions in the active regions, the non-radiative SRH recombination is approximately three times less in the micro-network nanostructures as compared to nanowires. The significantly reduced non-radiative recombination in the micro-network nanostructure explains their remarkably higher photoluminescence intensity as compared to the nanowires.

References

[1] A. Zhong, K. Hane, *Nanoscale Res. Lett.* **2012**, 7, 1.

[2] a) M. Kesaria, S. Shetty, S. M. Shivaprasad, *Cryst. Growth Des.* **2011**, 11, 4900; b) Y. Tamura, K. Hane, *Mater. Res. Bull.* **2016**, 83, 563; c) V. Thakur, M. Kesaria, S. M. Shivaprasad, *Solid State Commun.* **2013**, 171, 8.

[3] P. E. D. S. Rodriguez, P. Kumar, V. J. Gomez, N. H. Alvi, J. M. Manuel, F. M. Morales, J. J. Jimenez, R. Garcia, E. Calleja, R. Notzel, *Appl. Phys. Lett.* **2013**, 102, 1.

[4] a) D. Doppalapudi, S. N. Basu, J. K. F. Ludwig, T. D. Moustakas, *J. Appl. Phys.* **1998**, 84, 1389; b) M. G. Kibria, F. A. Chowdhury, S. Zhao, B. AlOtaibi, M. L. Trudeau, H. Guo, Z.Mi, *Nat. Commun.* **2015**, 6, 1.

[5] a) O. Ambacher, D. Brunner, R. Dimitrov, M. Stutzmann, A. Sohmer, F. Scholz, *Jpn. J. Appl. Phys.* **1998**, 37, 745; b) I. Vurgaftman, J. R. Meyer, *J. Appl. Phys.* **2003**, 94, 3675.

[6] X. Liu, S. Zhao, B. H. Le, Z. Mi, *Appl. Phys. Lett.* **2017**, 111, 1.